



UNIVERSITY OF LEEDS

This is a repository copy of *Improvement of the Stopband Spurious Window for a Dual-Mode Dielectric Resonator Filter by New Coupling Technique*.

White Rose Research Online URL for this paper:
<http://eprints.whiterose.ac.uk/130506/>

Version: Accepted Version

Article:

Luhaib, S orcid.org/0000-0002-6170-5114, Somjit, N orcid.org/0000-0003-1981-2618 and Hunter, IC orcid.org/0000-0002-4246-6971 (2018) Improvement of the Stopband Spurious Window for a Dual-Mode Dielectric Resonator Filter by New Coupling Technique. *International Journal of Electronics*, 105 (11). pp. 1805-1815. ISSN 0020-7217

<https://doi.org/10.1080/00207217.2018.1482008>

This article is under copyright. This is an Accepted Manuscript of an article published by Taylor & Francis in *International Journal of Electronics* on 29 May 2018, available online: <http://www.tandfonline.com/10.1080/00207217.2018.1482008>. Uploaded in accordance with the publisher's self-archiving policy.

Reuse

Items deposited in White Rose Research Online are protected by copyright, with all rights reserved unless indicated otherwise. They may be downloaded and/or printed for private study, or other acts as permitted by national copyright laws. The publisher or other rights holders may allow further reproduction and re-use of the full text version. This is indicated by the licence information on the White Rose Research Online record for the item.

Takedown

If you consider content in White Rose Research Online to be in breach of UK law, please notify us by emailing eprints@whiterose.ac.uk including the URL of the record and the reason for the withdrawal request.



eprints@whiterose.ac.uk
<https://eprints.whiterose.ac.uk/>



Improvement of the Stopband Spurious Window for a Dual-Mode Dielectric Reso

Journal:	<i>International Journal of Electronics</i>
Manuscript ID	TETN-2018-0061.R1
Manuscript Type:	International Journal of Electronics Letters (2500 word limit)
Date Submitted by the Author:	24-Apr-2018
Complete List of Authors:	Luhaib, Saad; University of Leeds School of Electronic and Electrical Engineering, Pollard Insitute Somjit , Nutapong; University of Leeds School of Electronic and Electrical Engineering, Pollard Institute Hunter, Ian; University of Leeds School of Electronic and Electrical Engineering, Pollard Institute
Keywords:	Filters, spurious window improvements, Dual-mode filters, Microwave, Waveguides
<p>Note: The following files were submitted by the author for peer review, but cannot be converted to PDF. You must view these files (e.g. movies) online.</p> <p>InteractAPALaTeX - Copy - Copy.7z</p>	

SCHOLARONE™
Manuscripts

ARTICLE TEMPLATE

Improvement of the Stopband Spurious Window for a Dual-Mode Dielectric Resonator Filter by New Coupling TechniqueSaad W. O. Luhaib^{a,b}, Nutapong Somjit^a and Ian C. Hunter^a^aSchool of Electronic and Electrical Engineering, University of Leeds, UK;^bElectrical Engineering Department, University of Mosul, Mosul, Iraq**ARTICLE HISTORY**

Compiled April 24, 2018

Abstract

This paper presents a new design technique for two configurations of a dual-mode filter using a dielectric loaded cavity operating at 1.95 GHz. The dielectric puck in the proposed filter was floated in the middle of a cylindrical metal cavity with short circuits on the side walls and holes through the ceramic from the side face. These holes allowed the insertion of coupling probes which did not affect the unloaded quality factor or the spurious window. The inline structure 4th pole Chebyshev dual mode filter offers a 870 MHz suppression window while the planar configuration was 710 MHz from the resonance frequency and the operation bandwidth of 54 MHz. The volume reduction ratio was eight times larger compared with a coaxial filter of the same Q factor.

KEYWORDS

Dual-mode filters; Dielectric resonator; Miniaturization of Bandpass filters

1. Introduction

Microwave dielectric resonator(DR) filters are widely employed in modern microwave communication systems due to their high Q-factor, temperature stability and compact size(Liang and Blair, 1998; Zhongxiang et al., 2011). Nowadays, the requirements of these filters are becoming more challenging because of the limitations in frequency spectrum and the high data rate demand. Single-mode resonators have been achieved to operate as DR filters with low loss in wireless systems (Cohn, 1968; Zaki and Chunming, 1986). Multi-mode DR filters offer a reduction of size without compromising the electrical performance (Mansour, 2004). In 1982, Fiedziuszko reported the first dual-degenerate mode in a dielectric-loaded cavity filter(Fiedziuszko, 1982), which allowed a size reduction ratio of 8.3% compared with standard TE_{111} . To further reduce the size, Mansour (Memarian and Mansour, 2009) proposed a new dielectric resonator configuration for size reduction consisting of a half cut cylindrical ceramic puck exhibiting dual mode performance at a certain D/L ratio. A four poles bandpass filter prototype was designed and measured with a spurious free window of 600 MHz and a 50% size reduction compared with HEH_{11} dual mode. One of the drawbacks of multi-mode DR filters is their poor spurious window which is less 300 MHz(Höft, 2010). A $TE_{11\delta}$ dual mode DR filter was presented by (Bakr et al., 2016) with a high

CONTACT Saad W. O. Luhaib. Email: elswol@leeds.ac.uk

1
2
3
4
5
6
7
8
9
10
11
12
13
14
15
16
17
18
19
20
21
22
23
24
25
26
27
28
29
30
31
32
33
34
35
36
37
38
39
40
41
42
43
44
45
46
47
48
49
50
51
52
53
54
55
56
57
58
59
60

Q factor. However, the coupling mechanism was poor, resulting in a reduction of the spurious window to about half what the eigen mode analysis predicted.

This paper presents a new coupling technique for a dual-mode loaded-cavity filter. The DR structure considers a dielectric puck situated in the middle of a metallic cavity and shorted on the sides. $TE_{11\delta}$ is the fundamental resonance for the dual-degenerate mode and HFSS simulations have been used to generate field patterns for this resonator and find the frequency response. Holes were provided through the middle side of the dielectric puck for the coupling I/O. The proposed resonator is ultra-compact in size with high unloaded Q-factor and broad spurious window. Planar and inline configurations of a 4th order dual mode chebyshev filter have been designed and simulated.

2. Resonator Configuration

Figure 1 shows the configuration of the $TE_{11\delta}$ dual mode DR. This consisted of a circular ceramic puck of high dielectric constant that had two perpendicular cylindrical holes bored in-plane with the cylindrical face in the middle of the cavity. The puck was suspended in the middle of a cylindrical metallic enclosure and short-circuited to the sidewalls, effectively miniaturizing the filter size while maintaining a good electrical performance. In the schematic, D and L are the diameter and length of the DR respectively and L_a is the distance above and below the ceramic puck and is filled with air. The term r_0 is the diameter of the holes cut through the dielectric which is done to improve the Q factor and make a good space for input/output coupling. The ceramic material used was barium titanate which has a permittivity of 43 and a loss tangent of 4×10^{-5} . This was placed in the metal cavity and short circuited on the side walls which had conductivity 4×10^7 S/m, while D=20mm, L=10mm and $L_a=5$ mm which are given the optimum value. The eigenmode solver in HFSS software was used to calculate the resonant frequency and unloaded Q factors for the DR proposed. Figure 2 illustrates the variation of the resonant frequency and Q factor of the first three modes against the radius of the hole r_0 .

$TE_{11\delta}$ and $TE_{21\delta}$ are dual mode. It can be seen that there is a slight increase in resonance frequency with an increase in r_0 . The maximum drift in frequency at mode $TE_{11\delta}$ is about 76 MHz and is doubled at the $TM_{01\delta}$ mode. Furthermore, the spurious free window is 720 MHz and still constant. For the same value of r_0 the Q factor does not affect the change in geometry for the second two modes, whilst, mode $TM_{01\delta}$ has been significantly decreased. It is clear that the TE mode was not affected by the size of the hole through the ceramic puck because it is parallel with the direction of the E-field. Figure 3 illustrates the pattern fields of the proposed cavity for the fundamental mode (1.96 GHz). From Figure 3, it can be observed that most of the E-field exists inside the dielectric puck surface which is distributed around the holes. Furthermore, the z-component of the E-field near to the hole could be used to control the coupling because the E-field is concentrated in the centre of the puck. The maximum H-field is distributed tangentially to the side of the puck, and shows the same performance in the dielectric with or without the added hole. The H-field was not significantly affected by the holes.

3. Design of the 4th Order Chebyshev Dual Mode Filter Planner Configuration

The procedure required to design a filter is as following:

- (1) Obtain the specification of the filter (resonance frequency f_r , Bandwidth (Bw), reflection loss (L_R).
- (2) Choose the appropriate topology of the filter.
- (3) Generate the coupling matrix of the filter.
- (4) Extract the coupling values.
- (5) Realization of the dimensions.

The next subsections will show all the coupling technique and associated calculations.

3.1. External Coupling

In order to achieve the external coupling for a dual mode dielectric resonator filter that has been proposed, a coaxial probe was oriented in the middle of the side hole through ceramic. E-field can be used for the coupling because it is maximum around the hole and perpendicular to the z-axis direction, as presented in Figure 3. The radius of the hole is 0.75 mm, which gave a resonant frequency of 1.96 GHz and Q_u of 3850. The external coupling can be calculated by the one-port method as equation shows (Hong , 2000).

$$Q_e = 0.5\pi f_0 \tau_D \quad (1)$$

where τ_D is the group delay in seconds at the resonance frequency f_0 . Figure 4 illustrates the external quality factors, Q_e , against the length of input/output probe (L_f). It can be observed that the L_f has a significant effect on the Q_e , which decreased with a rise in the L_f . A wide range of bandwidth can be achieved by adjusting the probe coupling.

3.2. Inter Resonator Coupling

The inter resonator coupling was implemented by a vertical etching-hole which is etched at 45° with respect to mode one and two. A circular hole acts as an impedance inverter over a broad bandwidth of the filter[5]. Lossy coupling probes were used to calculate the coupling bandwidth in the HFSS simulator. Figure 5 shows coupling bandwidth against the distance between the centre of the DR and the hole (X_f) with variations in the hole radius (r_e), measured in mm. It is observed that there are two distinct regions in the graph, below 6mm and over 8mm for X_f . The coupling bandwidths increased significantly when X_f increased for all of region one. However, the opposite is observed in region 2, where the coupling bandwidth decreased slowly with X_f . The maximum coupling bandwidth occurred at $X_f=7$ mm which is directly proportion to r_e with maximum value of 110 MHz at $r_e=3.6$ mm. Therefore, this coupling technique can be implemented as a filter with a variety of bandwidth from narrow to wideband.

3.3. Inter-Cavity Coupling

Connecting two cavities together entails an efficient and suitable configuration. In this filter, a coaxial probe was utilised in coupling the two cavities with a planar configuration as shown in Figure 7. A probe was placed in the centre of both DRs through the metallic wall. Figure 6 illustrates the inter-cavity coupling bandwidth against the length of the probe in each cavity (L_{f1}). It is noted that the L_{f1} has a significant effect on the coupling bandwidth. The coupling rose steadily in the range of L_{f1} (4 mm to 6 mm), increasing from 8 MHz to 32 MHz. It rapidly increased from 6 mm to 8 mm with about a 34 MHz/mm slope. Therefore, high accuracy is required to fabricate this filter.

4. Simulation Results

The configuration of the 4th order dual mode filter in HFSS software is shown in Figure 7. Two metallic cavities were used to present the filter with two pieces of ceramic ($\epsilon_r=43$ and $\tan \delta = 4 \times 10^{-5}$) placed in the middle and shorted by the side wall with conductivity= $4 \times 10^7 S/m$. The coaxial probe L_f was used for input/output coupling and L_{f1} controlled the inter-cavity coupling. The notch through the DR was used to present the inter-resonator coupling. To obtain the proper dimensions for all parameters as indicated in Figure. 7, it is essential to propose the topology of the filter and calculate the coupling matrix. The 4th order Chebyshev dual mode filter was designed with a centre frequency of 1.961 GHz, Bw of 52 MHz and L_R of 20 dB at the passband. We will use the coupling matrix as shown below.

$$M = \begin{bmatrix} S & 1 & 2 & 3 & 4 & L \\ S & 0 & 1.035 & 0 & 0 & 0 \\ 1 & 1.035 & 0 & 0.91 & 0 & 0 \\ 2 & 0 & 0.91 & 0 & 0.7 & 0 \\ 3 & 0 & 0 & 0.7 & 0 & 0.91 \\ 4 & 0 & 0 & 0 & 0.91 & 0 \\ L & 0 & 0 & 0 & 0 & 1.035 \end{bmatrix}$$

The input and output external quality factors and the coupling coefficients were computed for fractional bandwidth (FBW)=2.65% , and found to be $M_{12}=M_{34}= 47.35$ MHz, and $Q_e=35.19$. Referring to Figure 4, the length of the *I/O* probe to obtain the exact external quality factor was 7.4 mm; the internal coupling is shown in Figure 5. The dimension of the hole is 5 mm for the diameter and it was placed at 9.4 mm from the centre of the dielectric rod and the $M_{23}=36.4$ MHz with $L_{f1}=6.4$ mm. Figure 8 presents the S parameter response for the 4th order dual-mode DR filter at the designed values in HFSS. It can be observed that the bandwidth of the filter at -19 dB was equal to 54 MHz. The insertion loss at the resonant frequency (1.961GHz) is less than 0.25 dB and the extracted unloaded Q factor was slightly more than 3900. It is clear that the losses are much smaller than the filter with the direct contact coupling technique, because the tangential E-field at the probe is smaller. The maximum out of band rejection in the upper side is about 42 dB, which occurred at 2.125 GHz. The wideband response of the 4th order dual-mode DR filter is shown in Figure. 9 . It can be seen that the lower spurious mode appeared as a second order bandpass filter with

operated frequency about 2.67 GHz and bandwidth of 110 MHz. The first spurious frequency shifted down by 50 MHz compared with the eigen-mode analysis. Additionally, the high inter-resonator coupling for the dual-mode $TE_{21\delta}$ was similar and greater than the $TE_{11\delta}$ coupling, due to the pattern of the $TE_{21\delta}$. A single resonator in each cavity could be coupled by the inter-cavity coupling probe. The coupling to the $TM_{01\delta}$ mode (2.85 GHz) seems to be weak because the field pattern is not in the same direction with the I/O coupling probes. The cross coupling between $TE_{21\delta}$ and $TM_{01\delta}$ caused a transmission zero of about 2.85 GHz. The overall free spurious window was about 600 MHz, when was calculated from the 3 dB point of the first spurious band.

5. Design of 4th order Dual Mode Filter Inline Configuration

Inter-cavity couplings by using an iris plate between the two cavities are commonly used in waveguides and coaxial filters. The 4th order dual mode filter with an iris plate was proposed as shown in Figure. 10. It consisted of two pieces of ceramic with $\epsilon_r=43$ and $\tan \delta = 4 \times 10^{-5}$ placed in the middle and shorted to the side wall of the copper cavity $\sigma = 4 \times 10^7 S/m$. The hole through the ceramic was used for inter resonator coupling. The iris plate was used for the inter-cavity coupling and had a thickness of about 2 mm. The length L_x and width W_x of the iris controlled the coupling bandwidth between the two cavities. Figure. 11 illustrates the coupling bandwidth against L_x with varying values of W_x . It is clear that a linear proportion relationship exists between the coupling bandwidth and the L_x for a given value of W_x . Also, the slope increased further with W_x from 2 MHz/mm to 3.67 MHz/mm when W_x was changed from 1 mm to 4 mm. Furthermore, a good diversity of bandwidth can be achieved by adjusting the iris size as shown in Figure 11, in the range from 8 MHz to 50 MHz. The specification of the filter was similar to the 4th order Chebyshev planar structure. In this case, $f_0=1.961$ GHz, $Bw=52$ MHz and $L_R=20$ dB. Additionally, the filter topology, coupling matrix, I/O coupling length and inter resonator coupling were exactly the same as the previous case: the L_f , X_f and re are 7.4 mm, 2.5 mm and 9.4 mm respectively. $M_{23}=36.4$ MHz was realized from Figure 11, where L_x is 17 mm and W_x is 3 mm.

Figure 12 shows the S parameter response for the 4th order Chebyshev inline filter. It can be seen that the bandwidth of the filter at -19 dB was equal to 54 MHz. The insertion loss at the resonant frequency of 1.961 GHz was about 0.2 dB and the extracted unloaded Q factor was about 3800. It is clear that the losses were slightly higher than the filter with planar configuration; this may be caused by the tangential H-field crossing through the iris which has a thickness of 2 mm.

Figure 13 presents the wideband response of the 4th order Chebyshev dual-mode DR filter for iris structure and planar with patterned and unpatterned DR. It is observed that the maximum out-of-band rejection in the upper side is about 72 dB, which occurs at 2.4 GHz. The performance of the filter has a clean window of about 770 MHz under -40 dB. Moreover, the first spurious frequency at 2.67 GHz has been suppressed because the $TE_{21\delta}$ mode has a poor H-field in the middle of the iris which is perpendicular to the direction of the iris in this structure. The third mode, $TM_{01\delta}$, is a weak coupling of about -8 dB with a very narrow bandwidth at 2.83 GHz. Another reason, the probe is not reach to the middle of the cavity where is a high field of $TM_{01\delta}$, not much energy coupling could be collected. The spurious frequency occurred at 2.38 GHz for the unpatterned DR filter at the same conditions from (Bakr et al., 2016).

6. Conclusion

A new class of dual-mode loaded cavity filter was presented. The proposed resonator is ultra-compact in size with good electrical performance. Significant volume reduction ratio of 11% is achieved as compared to an air filled coaxial filter. Cutting holes through the ceramic in the middle of the cylindrical face does not affect the sequence of the modes in the DR. The inter resonator coupling was achieved by a hole on the ceramic placed at 45° w.r.t modes. Two 4th order Chebyshev dual mode filter were designed by using the planar and inline structures. The I/O Coupling was implemented by a probe connected with a 50Ω SMA connector. The planar configuration filter result provides a high Q-factor and good spurious window of about 600 MHz. Here, the inter-cavity coupling was achieved by a probe connected between the two cavities. The inline structure uses the iris for inter-cavity coupling, and shows a high suppression isolation which was about 770 MHz under -40 dB.

References

- Liang, X. F., and Blair, W. D. (1998) . High Q TE_{01} mode DR cavity filters for wireless base stations. *IEEE MTT-S International Microwave Symposium Digest*, Baltimore, MD, USA, 2, 825–828.
- Zhongxiang, Z., Chang, C., and Xianliang, W. (2011) . A compact cavity filter with novel TM mode dielectric resonator structure. *IEEE International Conference on Microwave Technology and Computational Electromagnetics*. Beijing, 111–113.
- Cohn, S. B. (1968). Microwave Bandpass Filters Containing High-Q Dielectric Resonators. *IEEE Transactions on Microwave Theory and Techniques*. 16(4), 218–227
- Zaki, K. A. and Chunming, C. (1986). New Results in Dielectric-Loaded Resonators. *IEEE Transactions on Microwave Theory and Techniques*. 34(7), 815–824.
- Mansour, R. (2004). Filter technologies for wireless base stations, *IEEE, Microwave Magazine*. 5(1), 68-74.
- Fiedziuszko, S. J. (1982). Dual-Mode Dielectric Resonator Loaded Cavity Filters. *IEEE Transactions on Microwave Theory and Techniques*. 30(9), 1311–1316.
- Memarian, M., and Mansour, R. (2009). Quad-mode and dual-mode dielectric resonator filters. *IEEE Transactions on Microwave Theory and Techniques*. 57(2), 3418–3426.
- Höft, M. (2010). Dielectric TE dual-mode resonator filters. *German Microwave Conference Digest of Papers*. Berlin, 206–209.
- Bakr, M. S., Luhaib, S. W. O., and Hunter, I. C. (2016). Novel Dielectric-Loaded Dual-Mode Cavity for Cellular Base Station Applications. *European Microwave Conference (EuMC)*. London. 763–766.
- Hong, J. S. (2000). Couplings of asynchronously tuned coupled microwave resonators. *IEE Proceedings - Microwaves, Antennas and Propagation*. 147(5), 354–358, Oct 2000.

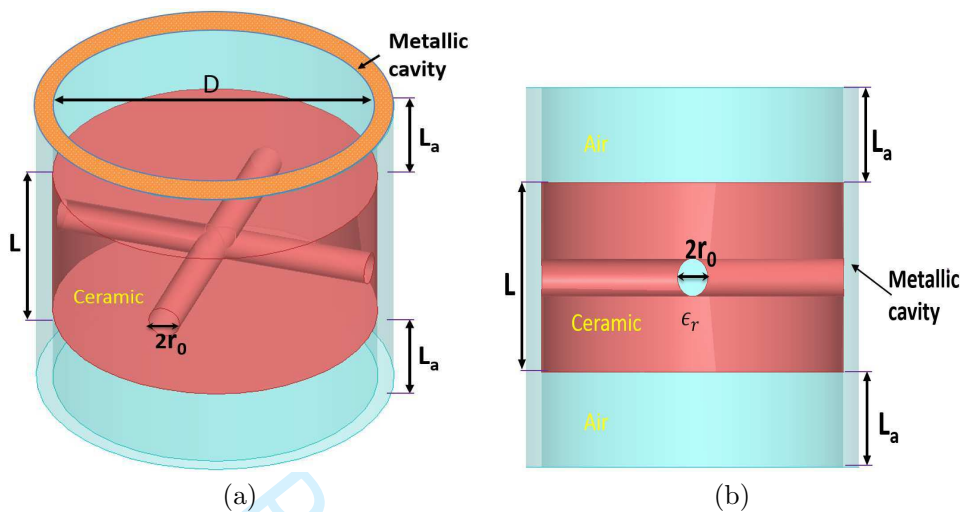


Figure 1. Configuration of dual mode dielectric resonator: (a) 3D view, (b) side view.

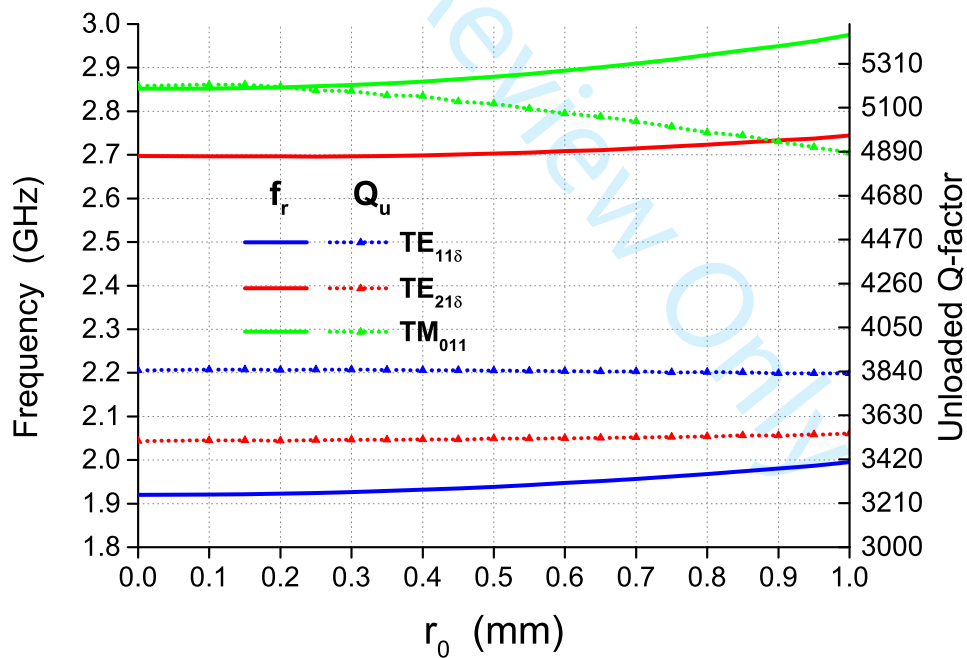


Figure 2. Resonance frequencies and Q_u with varying radius of hole (r_0).

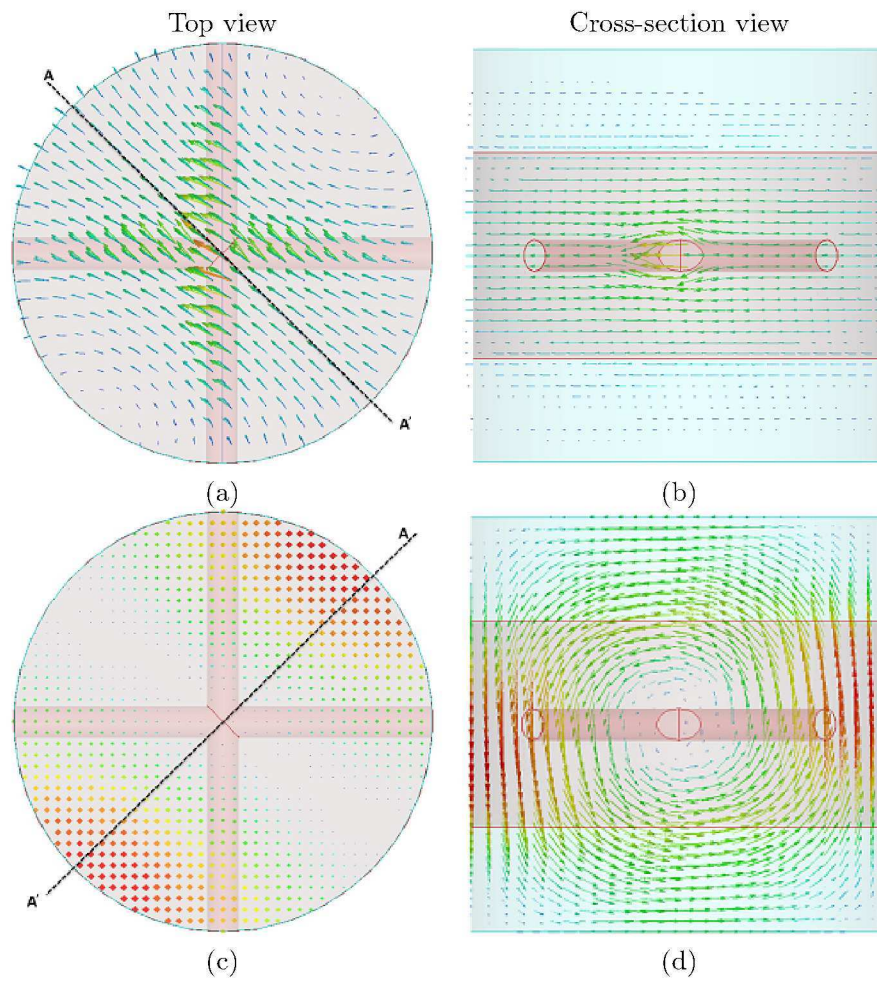


Figure 3. Field distributions of $TE_{11\delta}$ dual mode (a) and (b) E-field plot ,(c) and (d) H-field plot.

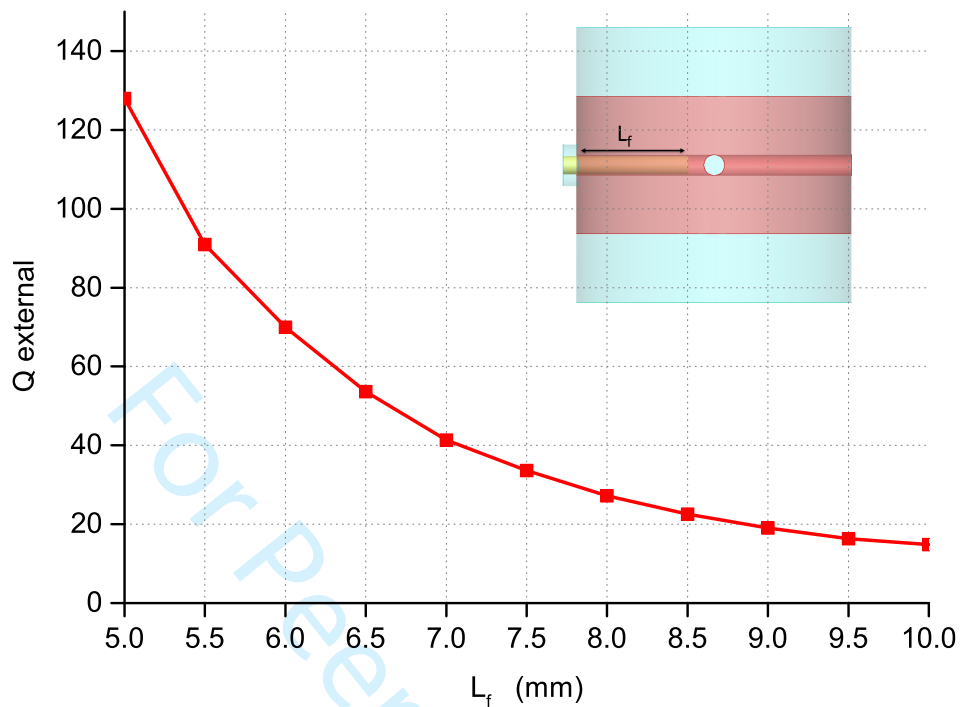


Figure 4. Variation of external quality factor (Q_e) against L_f .

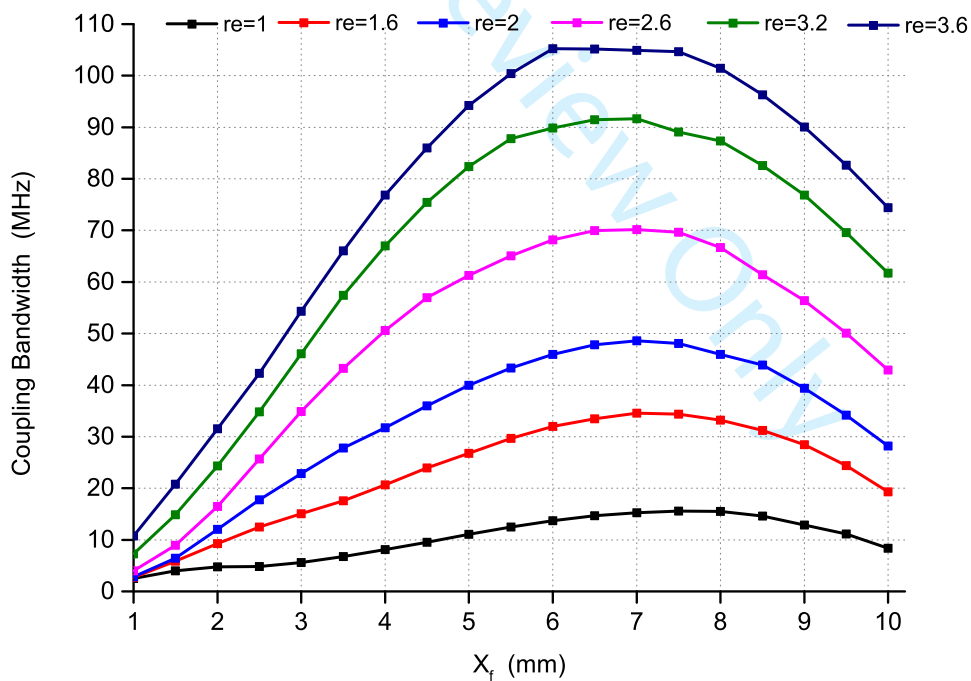


Figure 5. Coupling bandwidth varying with radius (re) and position of the hole (X_f).

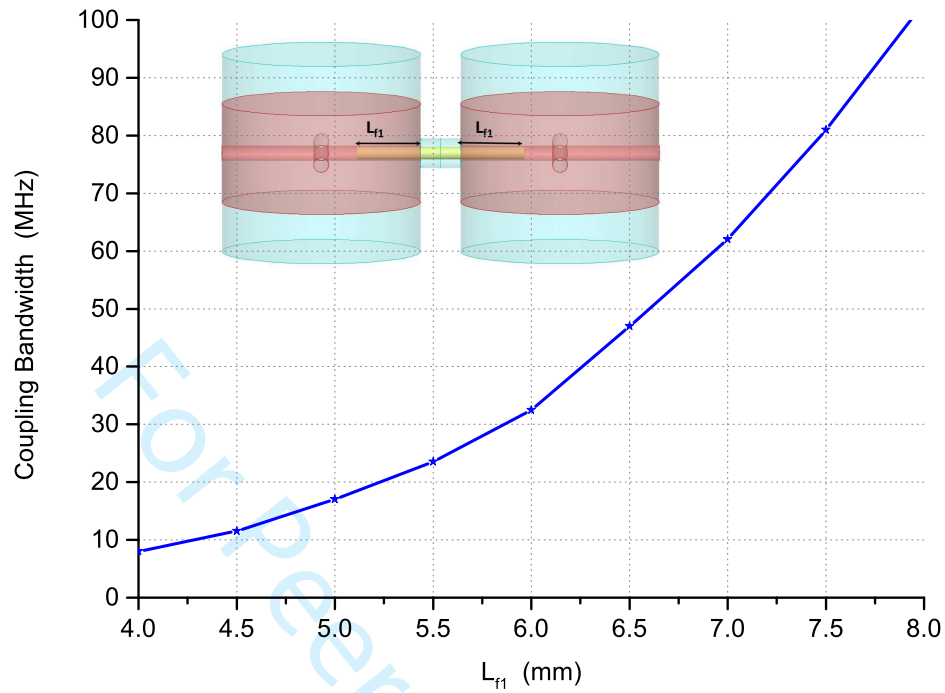


Figure 6. Variation of inter-cavity coupling (M_{23}) against L_{f1} .

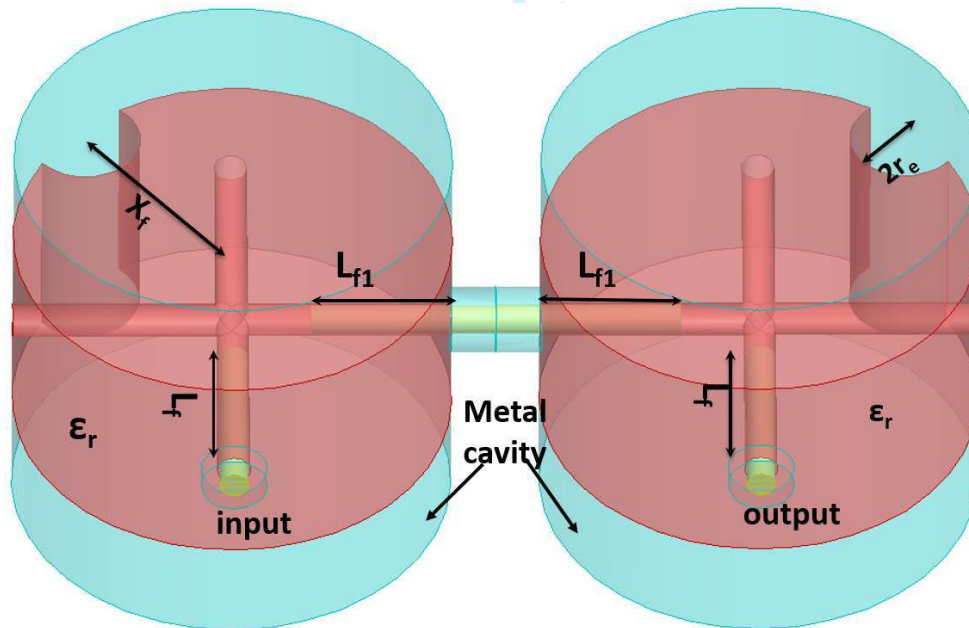


Figure 7. Configuration of 4th order filter dual mode in HFSS .

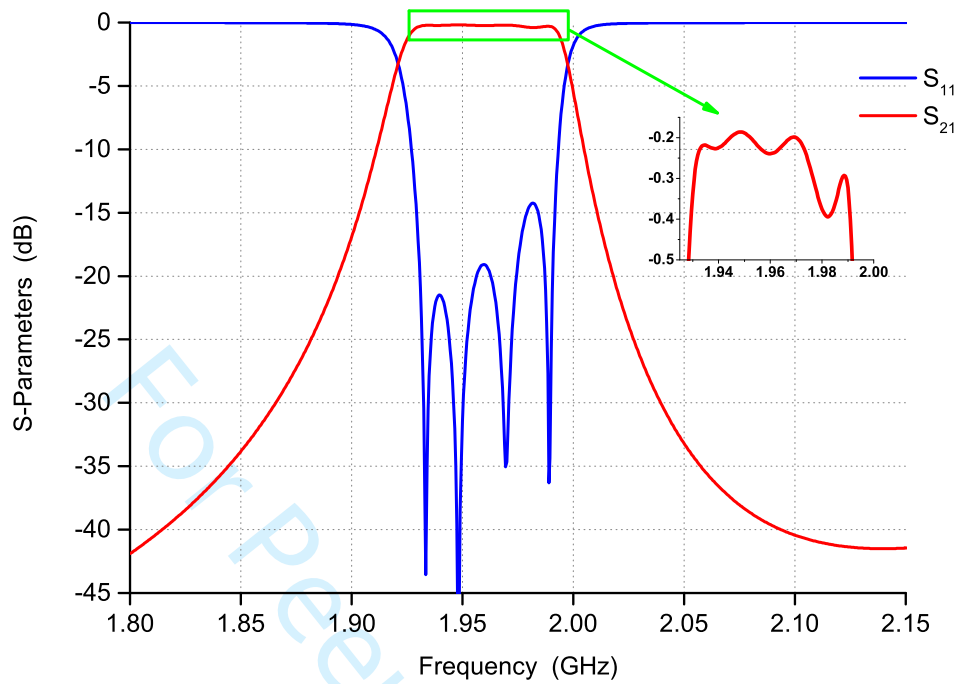


Figure 8. Simulated response of 4th order planar filter.

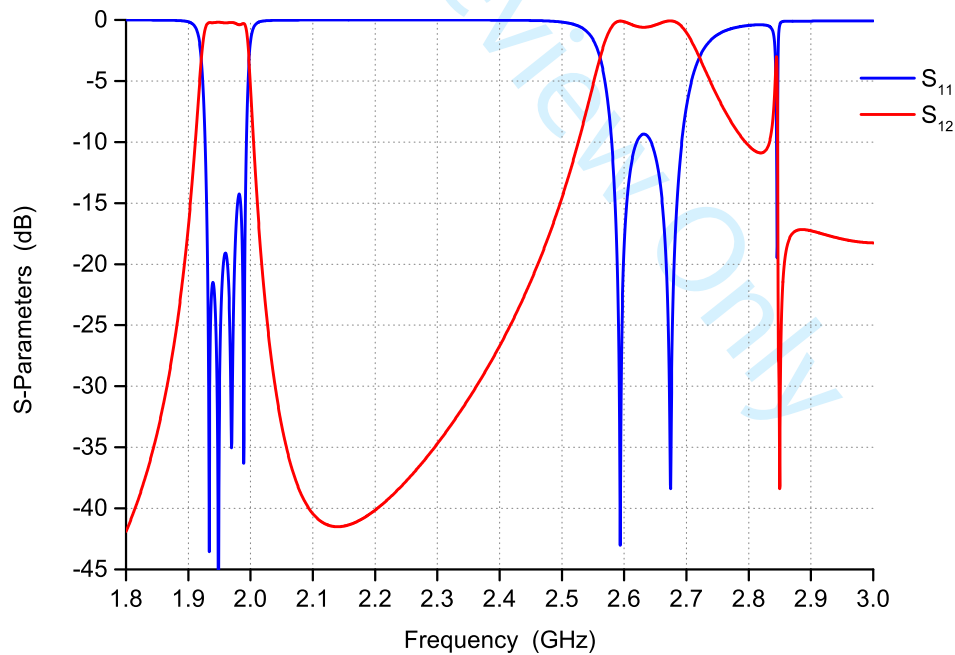


Figure 9. Simulated wideband response of 4th order planar filter.

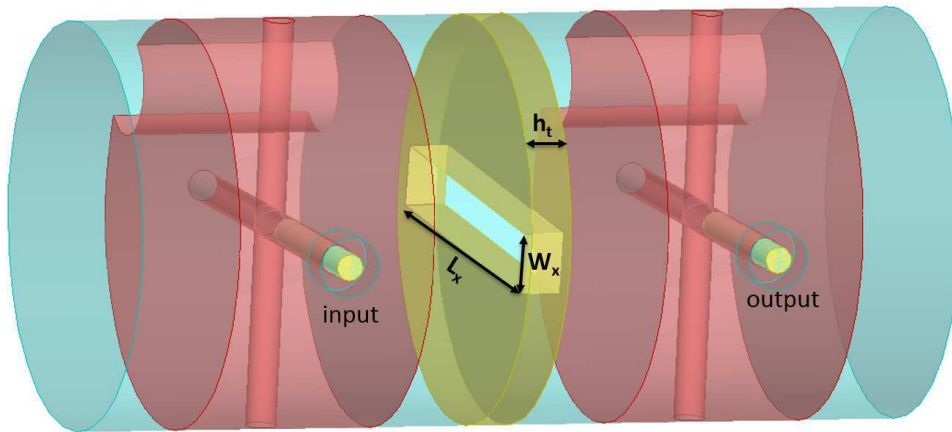


Figure 10. Inline configuration of 4th order filter dual mode in HFSS .

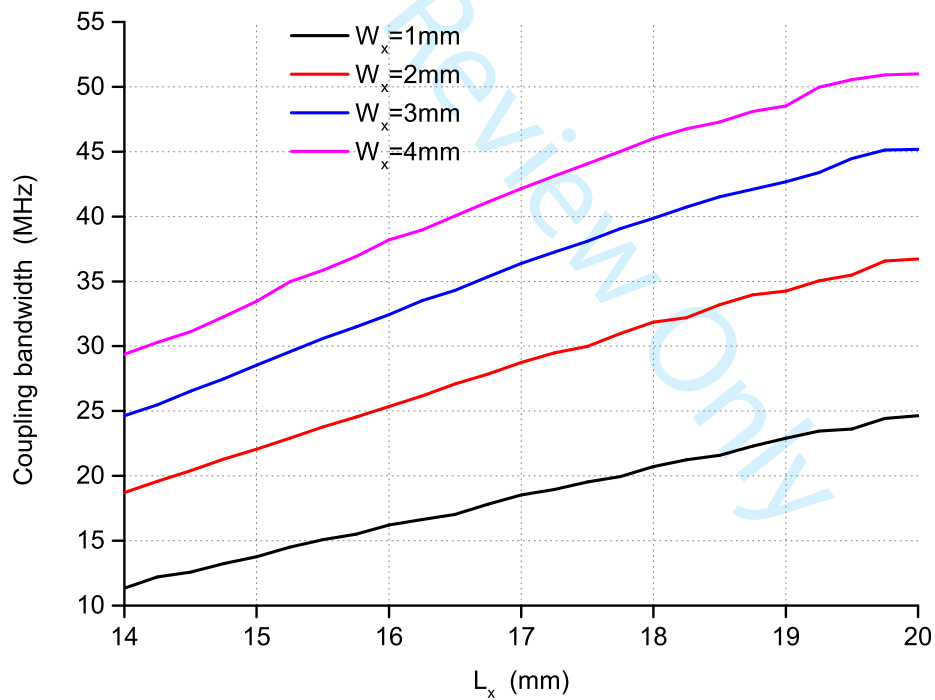


Figure 11. Coupling bandwidth for two cavities against L_x and W_x .

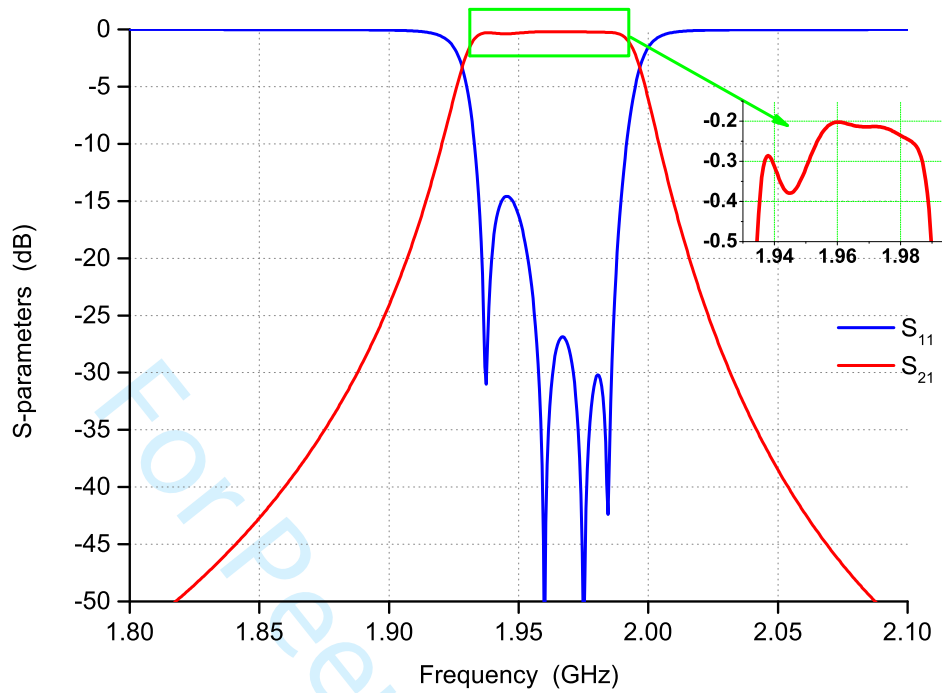


Figure 12. Simulated response of 4th order inline filter.

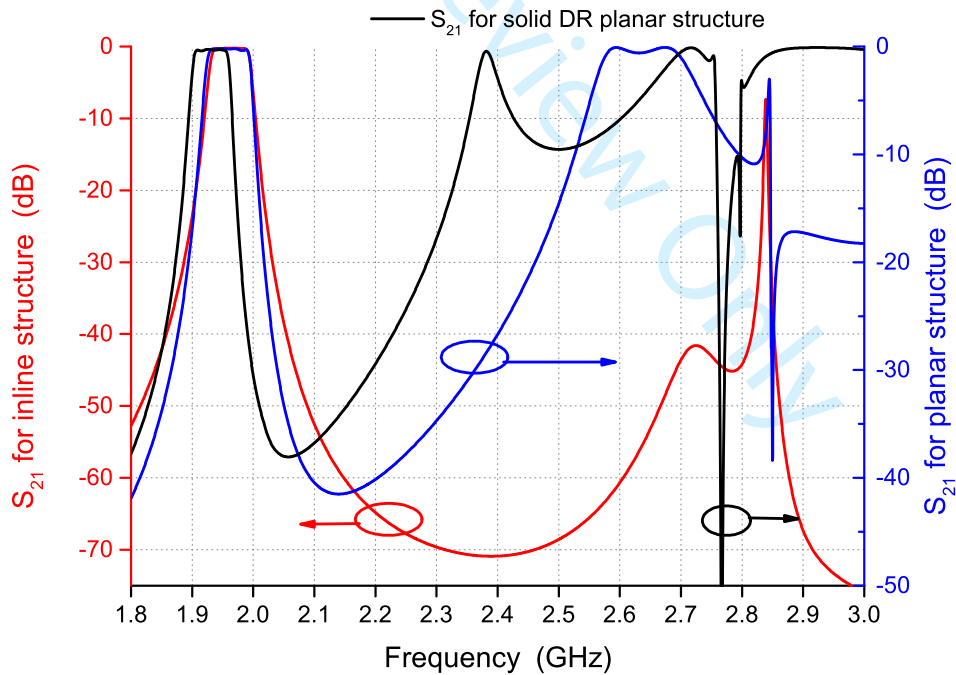


Figure 13. Simulated wideband response of 4th order inline filter.